Morphology and melt crystallization of poly(L-lactide) obtained by ring opening polymerization of L-lactide with zinc catalyst

Yong He, Zhongyong Fan, Jia Wei, Suming Li

Morphology and Melt Crystallization of Poly(L-lactide) Obtained by Ring Opening Polymerization of L-lactide With Zinc Catalyst

Yong He, Zhongyong Fan, Jia Wei, Suming Li
Department of Materials Science, Fudan University, Shanghai 200433, People's Republic of China

Suming Li
Research Center on Artificial Biopolymers, Faculty of Pharmacy, University Montpellier I, Montpellier 34060, France

The morphology and melt crystallization of zinc catalyzed poly(L-lactide) (PLLA) were investigated by using differential scanning calorimetry (DSC), polarized optical microscopy, and scanning electron microscopy. Isothermal melt crystallization performed at 95–135°C showed that the morphology depends on the degree of supercooling, as illustrated by crystallite perfection and lamellar thickening behaviors. Double melting peak was observed on DSC thermograms and attributed to the melt-recrystallization mechanism, small and imperfect crystals becoming gradually more stable ones. Circumferential and hexagonal cracks were detected in PLLA spherulites, which were formed during melt-crystallization at 135°C and quenching in liquid nitrogen. Rhythmic growth and thermal shrinkage are suggested to be the two main factors accounting for the formation of periodic cracks. Spherulite growth rates of PLLA were evaluated by using combined isothermal and nonisothermal procedures, and were analyzed by the secondary nucleation theory. The maximum growth rate reached 9.1 μm/min at 130°C. The temperature range investigated (120–155°C) belongs to the Regime II of crystallization. The value of U^* was found to be 1890 cal/mol, instead of 1500 cal/mol commonly used in literature, and K_g and σ were estimated to be 3.03×10^5 K^2 and 1.537×10^{-4} J/m^2, respectively. As a result, no distinct difference between PLLA catalyzed by zinc metal and those prepared with stannous octoate catalyst exists in this work. POLYM. ENG. SCI., 46:1583–1589, 2006. © 2006 Society of Plastics Engineers

INTRODUCTION

Degradable polymers have been attracting much attention for potential biomedical and environmental applications. As a typical degradable polyester, polylactide (PLA) can be used to fabricate various osteosynthetic devices, drug delivery systems, and tissue engineering scaffolds, etc. The degradation characteristics of PLA, which are of major importance for various applications, mainly depend on its morphology and crystallinity [1–3].

The crystallization and morphology of poly(L-lactide) (PLLA) have been extensively investigated [4–7]. Pennings et al. examined the morphology and crystal growth of PLLA as a function of molecular weight (MW) and degree of supercooling by using polarized optical microscopy (POM) equipped with a hot stage. The Hoffman and Lauritzen equation was applied to calculate the nucleation constants. Morphological changes from spherulites to axialites were observed at 163°C because of lower degree of supercooling [4]. Miyata et al. obtained the nucleation parameters of PLLA of different MW under various isothermal conditions. The maximal overall isothermal crystallization rate and spherulite growth rate were obtained at 105°C and at 120°C, respectively [5]. On studying the cold crystallization of amorphous PLLA, Kawaguchi et al. proposed the mechanism of phase transformation. The two exothermic peaks detected on differential scanning calorimetry (DSC) were attributed to the cold crystallization and phase transition from β form to α form. A multiple endothermic peak was observed by annealing samples between 105 and 120°C [6]. On the other hand, Iannace reported that the Regime II–III transition occurs below 115°C [7]. In this work, isothermal melt crystallization of PLLA was investigated in detail as a function of isothermal time, with particular attention paid to double melting behaviors.

The spherulite growth rate (G) is generally determined under isothermal conditions. At a specific temperature, the plot of spherulite radius (r) vs. isothermal time (t) is linear and the slope G can be expressed as:

$$G = \frac{dr}{dt}.$$

Nonisothermal procedure is also employed to obtain G by monitoring the growth of r as a function of temperature (T).

$$G = \frac{dr}{dT}\frac{dT}{dt}$$

where dr/dT is estimated from the first derivative of the r vs. T plot and dT/dt is the cooling rate as the spherulite growth front advances [8].

Experimental data of spherulite growth rate have been analyzed according to the secondary nucleation theory by Hoffman. The Hoffman and Lauritzen equation for the growth rate of a linear polymer crystal with folded chains is given by:

$$G = G_0 \exp\left[\frac{-U^*}{R\,(T_c - T_\infty)}\right] \exp\left(\frac{-K_g}{T_c\,\Delta T\, f}\right)$$

where K_g is the nucleation constant; ΔT is the degree of supercooling defined by $(T_m^0 - T_c)$; T_m^0 is the equilibrium melting point; T_c is crystallization temperature; f is a factor expressed as $2T_c/(T_m^0+T_c)$; U^* is the activation energy for segment diffusion to the crystallization site; R is the gas constant; T_∞ is the hypothetical temperature expressed as $(T_g - C)$ where all motion associated with viscous flow ceases, C is a constant (30–50 K); and G_0 is the front factor [9].

It is well known that the activation energy of linear PLLA is a specific parameter depending on the repetitional diffusion of chain segments. However, most authors used the assumed value of $U^* = 1500$ cal/mol, which gave good fit of the growth rate data for a number of polymers [4, 9, 10]. In this work, the method of the nonlinear least squares curve fitting is used to apply the Hoffman and Lauritzen equation to spherulite growth rate data of PLLA, and the values of U^* and K_g are determined.

Isothermal spherulite growth of PLLA has been investigated by many authors [11–14]. Tsuji et al. found that PLLA crystallizes in Regime II or Regime III kinetics depending on T_c if the number-average molecular weight (M_n) exceeds the critical values, and solely in Regime III kinetics for all the T_c with the M_n below critical values [11, 12]. They also investigated the spherulite growth of low MW PLLA [13]. On the other hand, Abe et al. reported that the transitions from Regime II to Regime I and from Regime III to Regime II occur at around 147°C and 120°C, respectively [14].

Stannous octoate and zinc metal are two commonly used catalysts or initiators in ring opening polymerization of lactides. The morphology and crystallization of PLLA initiated by stannous octoate have been investigated by many authors [4–7, 11–13]. Nevertheless, the presence of residues was suspected and indirectly shown, such as octanoyl moieties combined to some of the alcoholic chain ends, octanoic acid, and hydroxy tin octoate. Stannous octoate can be hardly removed from the chain ends, which could affect the structure and morphology of polymers [15]. In contrast, there are no chain end modifications in the case of zinc catalyzed PLLA, which is an ideal material for model studies of polymer crystallization and morphology [15, 16]. In this article, we report on melt crystallization behaviors, morphology, and spherulite growth rates of zinc catalyzed PLLA.

EXPERIMENTAL

Poly(L-lactide) (PLLA) was synthesized by ring opening polymerization of L-lactide using zinc metal as catalyst, according to the standard procedure reported by Vert et al. [16]. The obtained polymer was purified by the dissolution/precipitation method using dichloromethane as solvent and ethanol as nonsolvent to remove low molecular weight species and residual monomer. The weight-average molecular weight (M_w) of PLLA as determined by GPC is 1.36×10^5 g/mol, with a polydispersity index of 2.2. The rotatory power $[\alpha]_{20}^{D}$ measured in chloroform solution is −153°, which is consistent with literature data [17–19].

Differential scanning calorimetry (DSC) experiments were conducted by using a DuPont DSC 910 instrument calibrated with indium standard. Each sample of 5(±0.1) mg was scanned at a heating rate of 10°C/min under N_2 atmosphere after various thermal treatments. The summit of endothermic peak was taken as the melting temperature (T_m). In the process of isothermal melt crystallization, the samples were melted at 200°C for 3 min, rapidly cooled to the crystallization temperature, and then allowed to crystallize for 30 min.

Spherulite morphologies were examined with an Olympus model BH-2 polarized optical microscope (POM) and a Philips XL30 scanning electron microscope (SEM). The spherulite growth rate was measured by using a Leica DMLP POM equipped with a Linkam THMSE-600 hot stage. Thin films of PLLA were obtained by cold pressing under a pressure of 20 bars with an oil press of 769YP-15Z Model. Each sample was melted at 200°C between two slides, kept for 3 min to erase any thermal history, and then subjected to different thermal treatments after cooling from the melt at 50°C/min. The radius of growing crystals was monitored during crystallization with a video camera system taking photomicrographs automatically at appropriate time intervals. Dry nitrogen gas was applied throughout the hot stage.

RESULTS AND DISCUSSION

Melting Behaviors

Figure 1 shows the DSC thermograms of PLLA samples after various thermal treatments. The glass-transition tem-

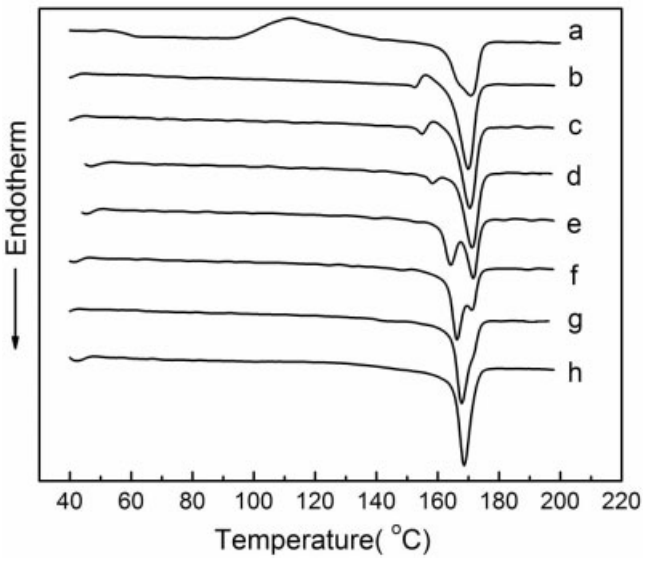

FIG. 1. DSC curves of various PLLA samples. (a) quenched after 2 min melting at 200°C; (b)–(h) isothermally melt crystallized for 30 min at 95, 100, 105, 110, 115, 120, 125°C, respectively.

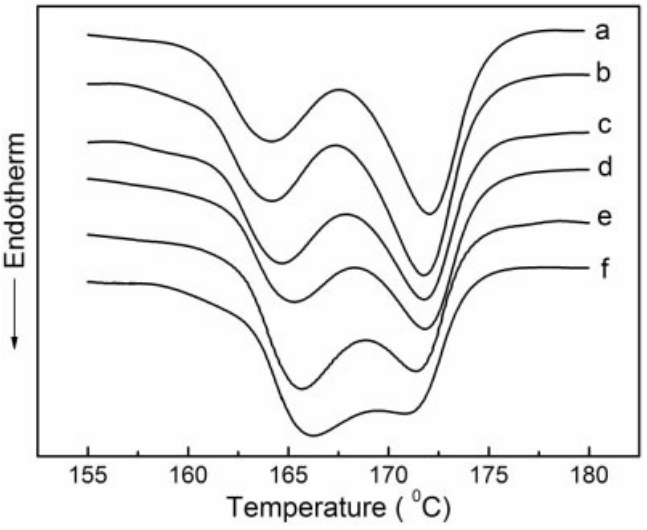

FIG. 2. DSC curves of PLLA after isothermal melt crystallization at 110°C for different time periods (a, 0.25 h; b, 0.5 h; c, 1 h; d, 4 h; e, 10 h; f, 24 h).

perature (T_g) of quenched PLLA is detected at 59.5°C with an enthalpy change of 34.5 J/kmol as estimated from heat flow change during the transition (curve a). The cold crystallization temperature ($T_{c,c}$) appears at 112.2°C and T_m at 170.8°C, in agreement with literature data [5, 6, 19, 20]. The melting endothermic enthalpy is about 48 J/g, which is equal to the exothermic enthalpy of cold crystallization. Various values of PLLA perfect crystal (ΔH_m^0) have been reported, ranging from 91 to 148 J/g [5, 21–25]. The value of 91 J/g reported by Wunderlich was used to obtain the degree of crystallinity (X_c), which is equal to 53% [22].

After melt crystallization at various temperatures, the glass transition and cold crystallization are hardly detectable (curves b–h). A small exothermic peak is detected between the two endothermic melting peaks for samples crystallized at 95 and 100°C (curves b, c), indicating that recrystallization occurs upon heating. A double melting peak is observed after melt crystallization at 105, 110, and 115°C (curves d, e, f). In the case of higher melt crystallization temperatures (120°C, 125°C), single melting peak appears (curves g, h).

Figure 2 shows the melting behavior of PLLA after melt crystallization at 110°C for various time periods up to 24 h. Two endothermic peaks are detected in each case, which are denoted as $T_{m,1}$ and $T_{m,2}$, respectively. With increasing isothermal time, $T_{m,1}$ shifts to higher temperature, while $T_{m,2}$ slightly decreases. The melting temperature and corresponding enthalpy data are presented in Table 1. It is noteworthy that the total melting enthalpy (ΔH_m) of PLLA, including both endothermic peaks, remains the same (*c.a.* 45 J/g) despite the isothermal time. In fact, with increasing isothermal crystallization time, initially formed small and imperfect crystals are subjected to crystal perfection and lamellar thickening. Therefore, $T_{m,1}$ corresponding to thickened lamellae increases, and the value of $\Delta H_{m,1}$ becomes higher. On the other hand, both $T_{m,2}$ and $\Delta H_{m,2}$ diminish due to less melt-recrystallization.

Double-melting behavior has been observed for many semicrystalline polymers, such as poly(ether ether ketone), poly(ethylene terephthalate), and iso-polystyrene (iPS) [26–29]. Melt-recrystallization model and dual lamellar thickness model have been proposed in the case of iPS [28, 29]. Yasuniwa et al. investigated the $T_{m,1}$ and $T_{m,2}$ dependence on the heating/cooling rates, suggesting that the melt-recrystallization mechanism be taken into account for the double melting behavior of PLLA [30].

When the degree of supercooling is relatively high (Fig. 1, curves b, c), the initially formed lamellae can hardly evolve because of the high transportation energy, resulting in a small endothermal peak of $T_{m,1}$ followed by melt-recrystallization. On the contrary, with lower degree of supercooling, almost perfect crystals are formed during melt crystallization, thus suppressing melt-recrystallization. As a consequence, a single melting endotherm is observed.

Cracks in PLLA Spherulites

An interesting phenomenon was observed by using POM and SEM: PLLA spherulites isothermally crystallized at

TABLE 1. Double melting temperature and enthalpy data of PLLA after melt crystallization at 110°C for various time periods.

Time (h)	$T_{m,1}$ (°C)	$T_{m,2}$ (°C)	ΔH_1 (J/g)	ΔH_2 (J/g)	ΔH_m (J/g)
0.25	164.0	172.1	21.1	24.5	45.6
0.5	164.2	171.9	21.2	24.2	45.4
1	164.8	171.8	24.2	20.5	44.7
4	165.1	171.8	29.1	17.0	46.1
10	165.7	171.5	31.3	13.9	45.2
24	166.1	171.4	36.8	9.2	46.0

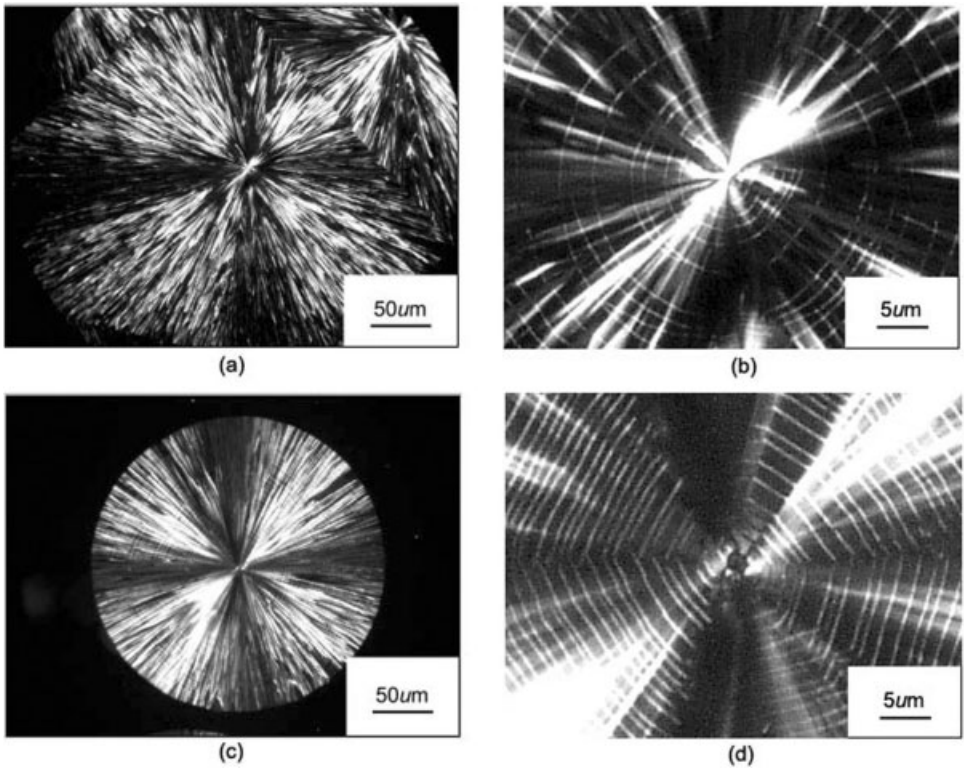

FIG. 3. Polarized optical micrographs of PLLA spherulites melt crystallized at 135°C. (a), (b) fine circles, (c), (d) hexagonal cracks.

135°C and quenched in liquid nitrogen exhibit circumferential and hexagonal cracks (Figs. 3 and 4). No extinction rings are visible on the spherulites, indicating that lamellae twisting and scrolling are not involved in the spherulite growth process, and consequently, are not related to the formation of the periodic cracks here [31]. In literature, optical micrographs exhibiting such cracks were obtained; however, no closer attention was paid to them [32, 33].

Similar patterns were reported for other polymers such as poly(3-hydroxybutyrate) (PHB) and poly(ethylene oxide) (PEO). Zhang et al. observed fine circles on banded spherulites of PHB, which were assigned to terraces resulting from the instability of the moving boundary of the melt film [34]. Terraces were also observed by Ding et al. in the case of PEO, which were formed at the front of the growing spherulites just before or exactly when two spherulites impinge on each other [35]. In other words, these fine and concentric circles were not related to lamellae organization in spherulites. In the case of our PLLA spherulites, however, the periodic cracks detected seem to be different from the fine circles or terraces of PHB and PEO.

Spiral and target patterns are common morphologies observed not only in excitable media and nonlinear dissipative systems, but also in polymeric, organic, and inorganic materials. It appears that the periodic cracks in PLLA spherulites present similar characteristics. Kyu et al. employed the time-dependent Ginzburg-Landau-equations model C (TDGL model C) to analyze the pattern forming aspects of polymer crystallization. The formation of spiral and target growth patterns in polymer spherulites was demonstrated theoretically and used to explain the twisted lamellar orientation [36]. In a recent article, Lotz and Cheng excluded the possibility that such spherulite growth features account for the twisted, untwisted, or scrolled lamellae. The authors considered unbalanced surface stresses as the origin of twisting and scrolling of polymer crystals [31]. Interest-

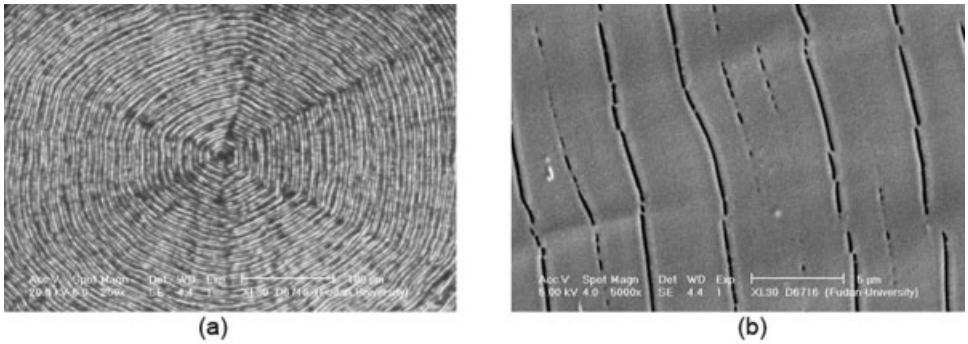

FIG. 4. SEM images of PLLA spherulites presenting hexagonal cracks obtained after melt crystallization at 135°C.

ingly, the theoretical simulation seems applicable to our results. In the case of PLLA, the periodic cracks formed in spherulites with no extinction rings are quite similar to the target patterns. It can be assumed that these cracks result from the rhythmic growth of target spherulites, as simulated by the phase-field TDGL model C. As crystalline-rich bands and amorphous-rich bands grow rhythmically, analogous to the theoretical simulation, the difference between those two bands induces formation of cracks on cooling process.

Subsequent investigations revealed that such regular and periodic cracks disappeared when cooling the spherulites at ambient temperature, although a few cracks were occasionally observed under unpolarized conditions. Therefore, the periodic cracks resulted from the shrinkage of spherulites on cooling process, which are different from terraces observed in the form of fine circles and extinction rings formed simultaneously with spherulite growth [34]. Different radial and circumferential thermal expansion coefficients that generate large stresses would be responsible for the occurrence of such cracks on cooling. Thermal shrinkage was previously proposed by Keller et al. to explain the cracks of PHB spherulites [37].

According to the arrangement of the crystallographic axes in the spherulites, the *b* axis is always radial, while *a* and *c* are tangential. While the thermal expansion coefficient along the *c* axis is negligible, there should be a difference between α_r, the thermal expansion coefficient along the *b* axis, and α_c concerning the *a* axis. Thus, a large tensile stress in the radial direction on cooling spherulites would induce circumferential or hexagonal cracking when α_r is higher than α_c.

With increasing spherulite radius, the outer cracks were gradually smoothed to become circumferential, the inner ones being hexagonal (see Fig. 4). These inner cracks might result from the (1,1,0) growth plane as hexagonal shaped crystals are formed at the early stage of melt crystallization at 135°C. Therefore, it can be concluded that rhythmic growth features and thermal shrinkage are the two main factors accounting for the formation of periodic cracks. It is noteworthy that these two factors have never been considered together to explain crystallization behaviors in literature. Further investigations are underway to better understand this phenomenon.

Spherulite Growth Rate (G) of PLLA

When a PLLA sample is cooled directly from the melt at 1°C/min, it would be difficult to obtain *G* values at high temperatures because of the long induction period prior to crystallization. A self-nucleation procedure was applied to enlarge the temperature range in the nonisothermal crystallization measurements. At first, the melted sample was cooled at 50°C/min to 130°C. Once the first spherulite was observed, the sample was heated up to 155°C at 50°C/min and kept for 1 min followed by cooling at 1°C/min. Figure 5 shows the variation of the spherulite radius as a function of temperature. The radius of the spherulite increases with

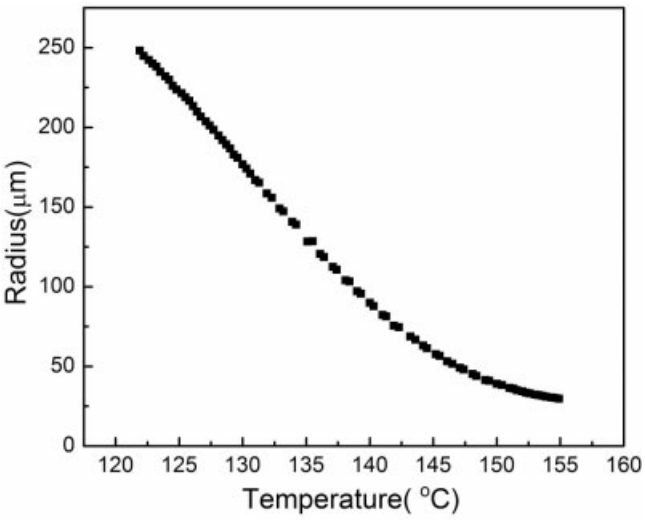

FIG. 5. Variation of the spherulite radius as a function of temperature during cooling at 1°C/min from 155 to 120°C after self-nucleation at 130°C.

decreasing temperature. *G* values were calculated by taking the first derivative of the *r* vs. *T* plot, according to the following formula:

$$G_i = -\frac{1}{2}\left(\frac{r_{i+1} - r_i}{T_{i+1} - T_i} + \frac{r_i - r_{i+1}}{T_i - T_{i-1}}\right).$$

The results were smoothed by adjacent-averaging and shown in Fig. 6. With decreasing crystallization temperature, the spherulite growth rate increased to attain a maximum value, $G_{max} = 9.1$ μm/min, at about 130°C and then decreased. The G_{max} value is larger than 5.1 μm/min and 6.7 μm/min, which were previously obtained respectively at

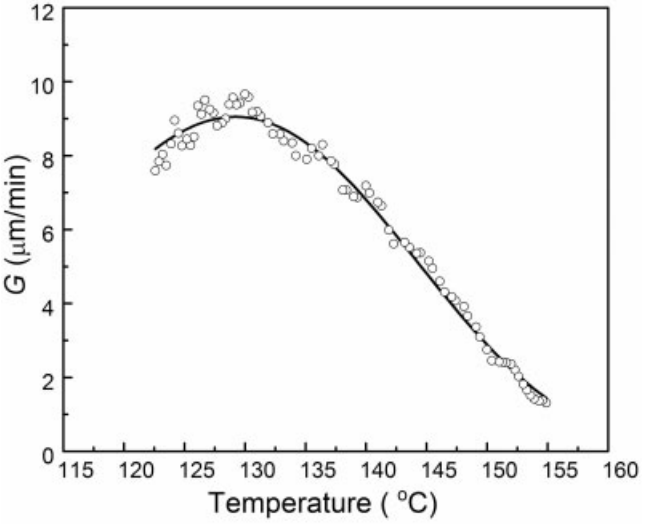

FIG. 6. Spherulite growth rates of PLLA calculated from data shown in Fig. 5 (shown as the dot) and fitted by the Hoffman and Lauritzen equation (shown as the line).

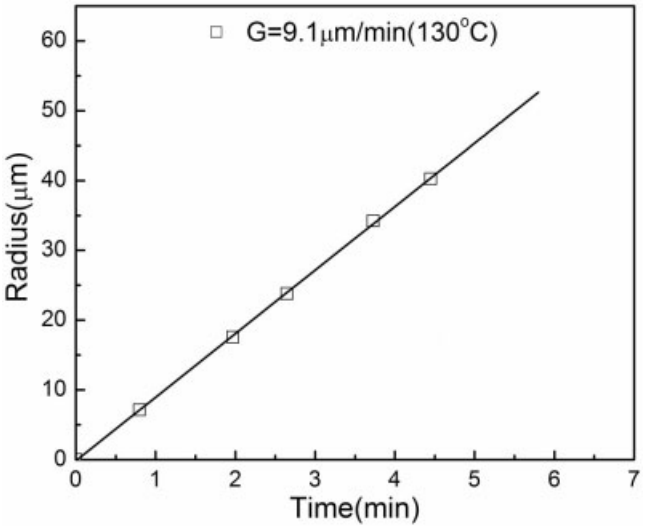

FIG. 7. Variation of the spherulite radius with time during isothermal crystallization at 130°C.

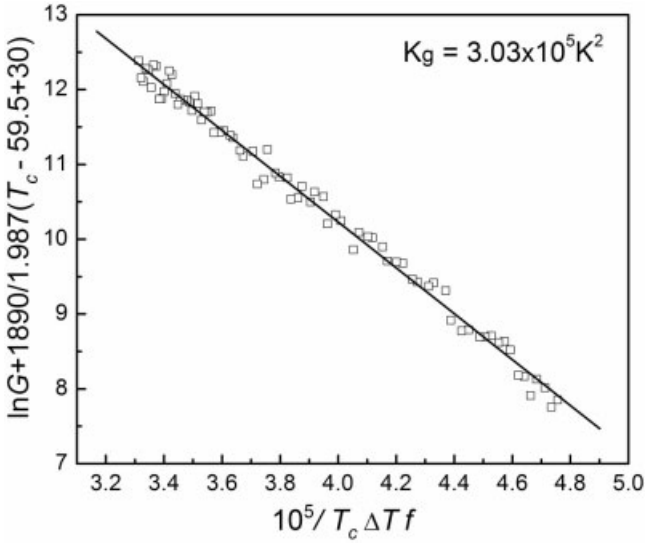

FIG. 8. Kinetic analysis of growth rate data of PLLA (U^* = 1890 cal/min, $T_\infty = T_g - 30$°C).

128°C in literature [4, 8]. Such a difference in growth rates could not be ascribed to the influence of molecular weights since all those samples possessed similar molecular weights. On the other hand, PLLA using zinc as catalyst has hydroxyl and carboxyl groups at both chain ends, while crystallization of stannous octoate catalyzed PLLA might be affected by the presence of octanoyl moieties at the chains ends. The higher crystallization temperature for and smaller chain ends could account for the higher G_{max} value obtained in this work.

G values were also obtained under isothermal conditions at specific temperatures (130, 140, 145°C). Figure 7 shows the radius growth as a function of time at 130°C, the slope of the plot giving the growth rate. G values of 9.1, 6.6, and 4.3 μm/min were obtained for crystallization at 130, 140, and 145°C, respectively. Therefore, spherulite growth rates determined by nonisothermal procedure are consistent with those by isothermal crystallization.

In the spherulite growth rate equation described by Hoffman and Lauritzen, we could set G_0, U^*, and K_g as three unknown parameters, T_c as the independent variable, G as the dependent variable. C equals to 30°C as an acceptable value according to previous reports, [4] T_m^0 = 207°C [4, 21], and T_g = 59.5°C. Nonisothermal procedure provided G values at various temperatures, which allowed us to obtain the defined parameters by using the method of the nonlinear least squares curve fitting. The fitting curve shown in Fig. 6 corresponds to the following parameter values: $G_0 = 5.1 \times 10^9$ μm/min, $U^* = 1890$ cal/mol, $K_g = 3.03 \times 10^5$ K^2.

Figure 8 presents the plot of $\ln G + U^*/R\,(T_c - T_\infty)$ vs. $1/(T_c \Delta T f)$, in which the U^* value was 1890 cal/mol, substituting the assumed value of 1500 cal/mol commonly used in literature [4, 7, 8]. The plot exhibits very good linearity, giving the same K_g value. There is no deflection in the plot, showing the absence of Regime I–II transition or Regime II–III transition. The value of K_g is in agreement with literature data, and the temperature range belongs to Regime II [4, 8].

In Regime II, K_g is defined as $(2b_0\sigma\,\sigma_e T_m^0/\Delta H_m^0 k)$, where b_0 is the layer thickness; σ is lateral surface energy; σ_e is fold surface free energy; ΔH_m^0 is heat of fusion per unit volume, and k is the Boltzmann constant. Using the values reported in literature [38], $b_0 = 0.517$ nm, $\Delta H_m^0 = 1.11083 \times 10^8$ J/m^3, $\sigma_e = 6.089 \times 10^{-4}$ J/m^2, the σ value is obtained ($\sigma = 1.537 \times 10^{-4}$ J/m^2), which is higher than that reported in literature ($\sigma = 1.203 \times 10^{-4}$ J/m^2) [4, 38].

CONCLUSIONS

Isothermally melt crystallization of PLLA synthesized by using zinc catalyst was studied with different degrees of supercooling at 95–135°C. The results showed that the morphology depends on the degree of supercooling, as illustrated by crystallite perfection and lamellar thickening behaviors. Double melting peak was attributed to the melt-recrystallization mechanism, small and imperfect crystals becoming gradually more stable ones. It was also found that the whole endothermal enthalpy remained the same as the lower melting peak turned to be larger with increasing isothermal time.

Circumferential and hexagonal cracks observed in PLLA spherulites were examined. Rhythmic growth and thermal shrinkage are identified as the two main factors accounting for the formation of periodic cracks.

Isothermal and nonisothermal procedures were combined to evaluate the variation of spherulite growth rate with crystallization temperature. The maximum G value is about 9.1 μm/min, which is higher than those reported in literature. The data were analyzed by using the secondary nucleation theory. The method of the nonlinear least squares curve fitting was employed, directly giving the value of U^*.

And crystallization at the temperature range (120°C −155°C) belongs to Regime II, with $U^* = 1890$ cal/mol, $K_g = 3.03 \times 10^5$ K^2, and $\sigma = 1.537 \times 10^{-4}$ J/m^2.

ACKNOWLEDGMENTS

The authors thank Professor Rongshi Cheng at Nanjing University for the use of POM equipment and valuable discussions.

REFERENCES

1. M. Vert, S.M. Li, G. Spenlehauer, and P. Guerin, *J. Mater. Sci. Mater. Med.*, **3**, 432 (1992).
2. M. Vert, G. Schwarch, and J. Coudane, *J. Macromol. Sci. Pure Appl. Chem. A*, **32**, 787 (1995).
3. S. Gogolewski, *Clin. Mater.*, **10**, 13 (1992).
4. R. Vasanthakumari and A.J. Pennings, *Polymer*, **24**, 175 (1983).
5. T. Miyata and T. Masuko, *Polymer*, **39**, 5515 (1998).
6. Y. Ohtani, K. Okumura, and A. Kawaguchi, *J. Macromol. Sci. Phys.*, **42**, 875 (2003).
7. S. Iannace and L. Nicolais, *J. Appl. Polym. Sci.*, **64**, 911 (1997).
8. M.L. Di Lorenzo, *Polymer*, **42**, 9441 (2001).
9. J.D. Hoffman, *Polymer*, **24**, 3 (1983).
10. D.P. Fletcher and J. Klein, *Polym. Commun.*, **26**, 2 (1985).
11. H. Tsuji, T. Miyase, Y. Tezuka, and S.K. Saha, *Biomacromolecules*, **6**, 244 (2005).
12. H. Tsuji, Y. Tezuka, S.K. Saha, M. Suzuki, and S. Itsuno, *Polymer*, **46**, 4917 (2005).
13. H. Tsuji and Y. Tezuka, *Biomacromolecules*, **5**, 1181 (2004).
14. H. Abe, Y. Kikkawa, Y. Inoue, and Y. Doi, *Biomacromolecules*, **2**, 1007 (2001).
15. G. Schwach, J. Coudane, R. Engel, and M. Vert, *J. Polym. Sci. Polym. Chem.*, **35**, 3431 (1997).
16. M. Vert, F. Chabot, J. Leray, and P. Christel, French Patent, 7,829,978 (1978).
17. N. Yui, P.J. Dijkstra, and J. Feijen, *Die Makromolekulare Chemie.*, **191**, 481 (1990).
18. A.E. Tonelli and P.J. Flory, *Macromolecules*, **2**, 225 (1969).
19. J.R. Sarasua, R.E. Prud'homme, M. Wisniewski, A. Le Borgne, and N. Spassky, *Macromolecules*, **31**, 3895 (1998).
20. D. Garlotta, *J. Polym. Environ.*, **9**, 63 (2001).
21. E.W. Fisher, H.J. Sterzel, and G. Wegner, *Kolloid Z. u. Z. Polymere*, **251**, 980 (1973).
22. M. Pyda, R.C. Bopp, and B. Wunderlich, *J. Chem. Therm.*, **36**, 731 (2004).
23. D. Cohn, H. Younes, and G. Marom, *Polymer*, **28**, 2018 (1987).
24. D.K. Gilding and A.M. Reed, *Polymer*, **20**, 1459 (1979).
25. G.L. Loomis, J.R. Murdoch, and K.H. Gardner, *Polym. Prepr.*, **39**, 55 (1990).
26. P. Srimoaon, N. Dangseeyun, and P. Supaphol, *Eur. Polym. J.*, **40**, 599 (2004).
27. S. Tan, A. Su, W. Li, and E. Zhou, *J. Polym. Sci. Part B: Polym. Phys.*, **38**, 53 (2000).
28. T. Liu, S. Yan, M. Bonnet, I. Lieberwirth, K.D. Rogausch, and J. Petermann, *J. Mater. Sci.*, **35**, 5047 (2002).
29. T. Liu and J. Petermann, *Polymer*, **42**, 6453 (2001).
30. M. Yasuniwa, S. Tsubakihara, Y. Sugimoto, and C. Nakafuku, *J. Polym. Sci. Polym. Chem.*, **42**, 25 (2004).
31. B. Lotz and S.Z.D. Cheng, *Polymer*, **46**, 577 (2004).
32. H. Tsuji and Y. Ikada, *Macromolecules*, **26**, 6918 (1993).
33. M. Gazzano, M.L. Focarete, C. Riekel, and M. Scandola, *Biomacromolecules*, **5**, 553 (2004).
34. J. Xu, B. Guo, G. Chen, and Z. Zhang, *J. Polym. Sci. Part B: Polym. Phys.*, **41**, 2128 (2003).
35. J.D. Ding, J.X. Zhu, and Y.L. Yang, *Chem. J. Chin. Univ. Chin.*, **17**, 498 (1996).
36. T. Kyu, H.W. Chiu, A.J. Guenthner, Y. Okabe, H. Saito, and T. Inoue, *Phys. Rev. Lett.*, **83**, 2749 (1999).
37. P.J. Barham and A. Keller, *J. Mater. Sci. Lett.*, **8**, 490 (1989).
38. K. Kishore and R. Vasanthakumari, *Colloid Polym. Sci.*, **266**, 999 (1988).